Diameter- and Metallicity-Selective Enrichment of Single-Walled Carbon Nanotubes Using Polymethacrylates with Pendant Aromatic Functional Groups

ARTICLE *in* SMALL · JUNE 2010

Impact Factor: 8.37 · DOI: 10.1002/smll.200902415 · Source: PubMed

small NANO MICRO

Diameter- and Metallicity-Selective Enrichment of Single-Walled Carbon Nanotubes Using Polymethacrylates with Pendant Aromatic Functional Groups

*Xiaoyong Pan, Lain-Jong Li, and Mary B. Chan-Park**

Current methods for the synthesis of single-walled nanotubes (SWNTs) produce mixtures of semiconducting (sem-) and metallic (met-) nanotubes. Most approaches to the chemical separation of sem-/met-SWNTs are based on small neutral molecules or conjugated aromatic polymers, which characteristically have low separation/dispersion efficiencies or present difficulties in the postseparation removal of the polymer so that the resulting field-effect transistors (FETs) have poor performance. In this Full Paper, the use of three polymethacrylates with different pendant aromatic functional groups to separate cobalt–molybdenum catalyst (CoMoCAT) SWNTs according to their metallicity and diameters is reported. UV/Vis/NIR spectroscopy indicates that poly(methyl-methacrylate-co-fluorescein-o-acrylate) (PMMAFA) and poly(9-anthracenylmethyl-methacrylate) (PAMMA) preferentially disperse semiconducting SWNTs while poly-(2-naphthylmethacrylate) (PNMA) preferentially disperses metallic SWNTs, all in dimethylforamide (DMF). Photoluminescence excitation (PLE) spectroscopy indicates that all three polymers preferentially disperse smaller-diameter SWNTs, particularly those of (6,5) chirality, in DMF. When chloroform is used instead of DMF, the larger-diameter SWNTs (8,4) and (7,6) are instead selected by PNMA. The solvent effects suggest that diameter selectivity and change of polymer conformation is probably responsible. Change of the polymer fluorescence upon interaction with SWNTs indicates that metallicity selectivity presumably results from the photon-induced dipole–dipole interaction between polymeric chromophore and SWNTs. Thin-film FET devices using semiconductor-enriched solution with PMMAFA have been successfully fabricated and the device performance confirms the sem-SWNTs enrichment with a highly reproducible on/off ratio of about 10^3.

Keywords:
- metallicity
- semiconductors
- single-walled carbon nanotubes
- transistors

[*] X. Pan, M. B. Chan-Park
School of Chemical and Biomedical Engineering
Nanyang Technological University
62 Nanyang Drive, Singapore 637459 (Singapore)
E-mail: mbechan@ntu.edu.sg

L.-J. Li
School of Materials Science and Engineering
Nanyang Technological University
62 Nanyang Drive, Singapore 637459 (Singapore)

Supporting Information is available on the WWW under http://www.small-journal.com or from the author.

DOI: 10.1002/smll.200902415

1. Introduction

Since their discovery by Iijima in 1991,[1] single-walled carbon nanotubes (SWNTs) have been the subject of much interest as one of the best candidate new materials for electronic devices,[2–6] owing to their exceptional conductivity and field-effect transistor (FET) behavior. However, an unsolved obstacle to the realization of their widespread application is the control of nanotube chirality. During nanotube growth processes, many possible chiralities will be produced and about a third of the produced nanotube species are metallic (met-SWNTs) and the rest are semiconducting (sem-SWNTs).[7,8] Only sem-SWNTs are desired for use as the FET active material. The poor growth selectivity of sem-SWNTs[9] and the low efficiency of the destruction of met-SWNTs[10,11] make efficient postsynthesis separation schemes necessary.

Although the techniques of alternating-current dielectrophoresis,[12–14] anion-exchange chromatography of DNA-wrapped carbon nanotubes,[15,16] and density-gradient centrifugation method,[17] and so on have been successfully employed in the separation of met- and sem-SWNTs, the difficulty of scale up limits their application. Chemical methods, which can be classified into covalent[18–22] and noncovalent functionalization,[23–27] are more easily scalable and therefore more attractive separation techniques. Noncovalent approaches are particularly interesting because they are able to preserve nearly all of the intrinsic properties of the SWNTs.

The selective precipitation of met-SWNTs by adhesion of small molecules, such as octadecylamine[24] and bromine,[25] has been successfully reported but these methods still achieve only limited selectivity. In both cases, selective adsorption occurs when the molecules are adsorbed on the sidewalls of the SWNTs via weak linkages similar to hydrogen bonding. Recently, flavin mononucleotide[28] has been demonstrated to be highly effective for chirality-selective enrichment and intermolecular hydrogen bonding plays a critical role in the selectivity. Alternatively, the extended π-electron system in SWNTs can associate strongly with other π-electron systems, such as those of aromatic molecules, via π–π stacking interactions.[29–33] Experiments have proved the feasibility of pyrene derivatives[34] or conjugated aromatic polymers[35–37] to selectively suspend certain SWNT species. However, the poor dispersion capability of the small neutral pyrene-derivative molecules limits their efficacy and the strong π–π interaction between SWNTs and the conjugated aromatic polymers[35–37] due to their large stacking areas hinders postenrichment removal of the polymers. In addition, the strong π–π interaction may to some extent hinder the adjustment of the conformation of the polymers on the SWNT sidewall, thus decreasing the separation efficiency.

In this investigation, three novel polymethacrylates with different pendant aromatic functional groups, poly(2-naphthylmethacrylate) (PNMA), poly(methyl-methacrylate-*co*-fluorescein-*o*-acrylate) (PMMAFA), and poly(9-anthracenylmethyl methacrylate) (PAMMA) (Figure 1), were investigated for their selectivity in SWNT separation. Compared with conjugated aromatic polymers, these polymers have a lower contact area between the pendant aromatic groups and the SWNT sidewalls so that it is easier to remove the separating agent after separation. The flexible polymethacrylate backbone assists SWNT solvation in common organic solvents, while the large pendant aromatic structures have a strong affinity to the SWNTs. The SWNTs studied were synthesized by the cobalt–molybdenum catalyst (CoMoCAT) process. UV/Vis/near-infrared (UV/Vis/NIR) spectra and photoluminescence excitation maps (PLE) were used to measure the degree of met/sem dispersion and chiral-species selectivity. The influence of the solvent on selectivity was explored. In addition, the change of the polymer fluorescence upon interaction with SWNTs was tracked. High enrichment of sem-SWNTs was confirmed in FET devices.

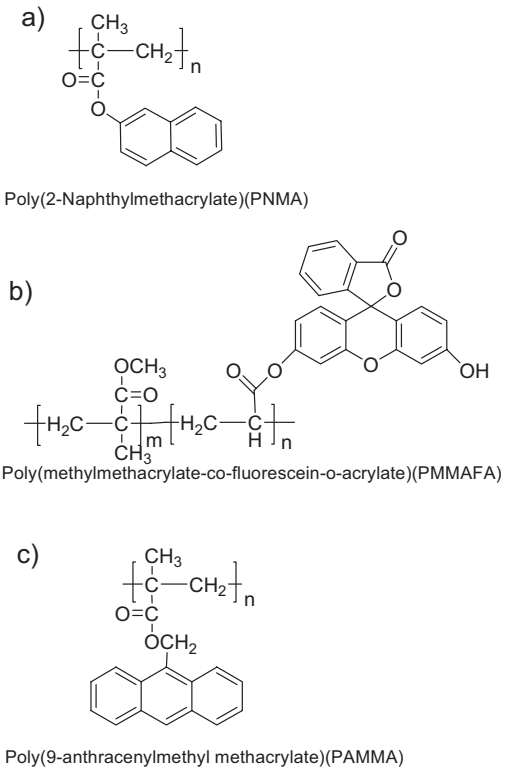

Figure 1. Structures of the polymers used in this study.

2. Results and Discussion

2.1. UV/Vis/NIR spectra

UV/Vis/NIR absorption spectra of postseparation suspended and precipitated SWNTs for all polymers are shown in Figure 2. Also shown are the absorbance spectra of the SWNTs dispersed in D_2O solution using the ionic sodium dodecylbenzenesulfonic acid (SDBS) surfactant, which is assumed to disperse SWNTs without any species preference.

The optical absorbance spectra can tentatively be used to estimate the SWNT-species content of the samples since the peak intensities are approximately proportional to the concentrations of the dispersed species. The spectra contain spectroscopic signatures of the interband electronic transitions corresponding to the M_{11} band of met-SWNTs and the S_{11} and S_{22} bands of sem-SWNTs.

NANO MICRO small

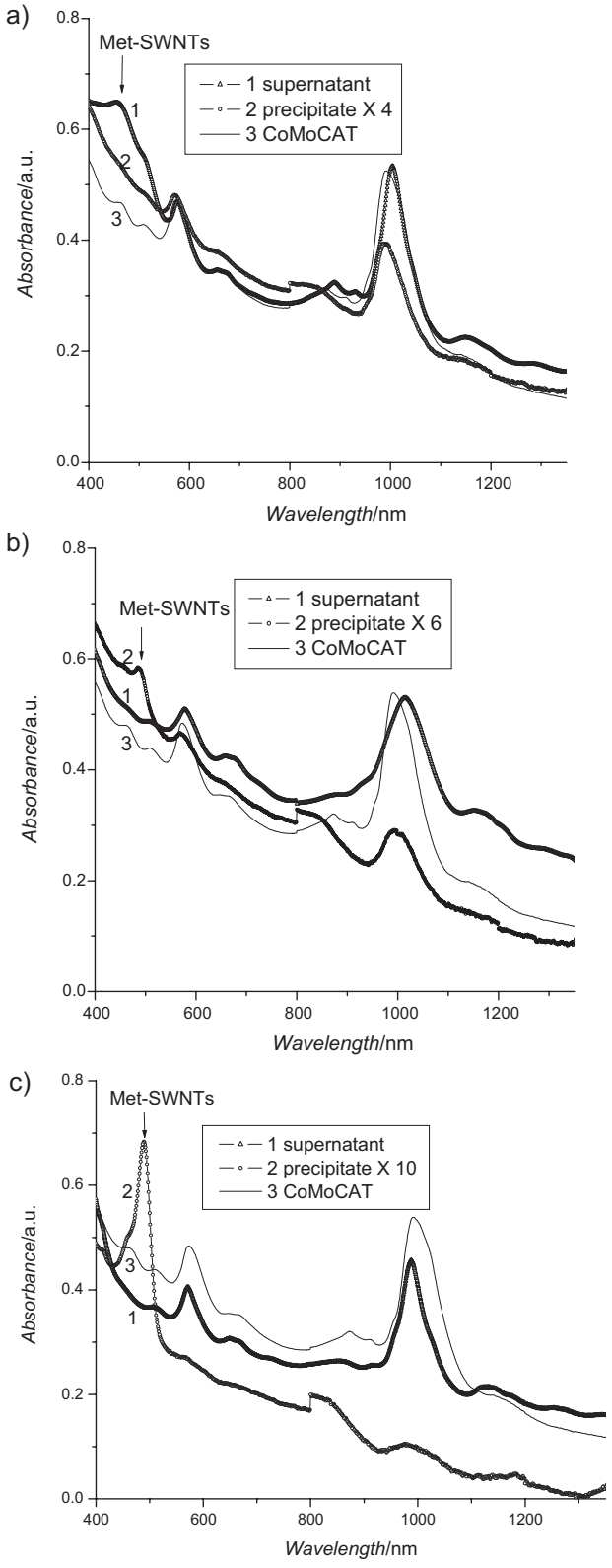

Figure 2. UV/Vis/NIR absorbance spectra of chemically separated SWNTs. CoMoCAT-produced SWNTs in DMF with a) PNMA, b) PMMAFA, and c) PAMMA. (Note: Line 3 is the spectra of the ''as-received'' SWNTs dispersed in D_2O/SDBS solution.)

All separations were performed with the same process parameters, including sonication power and time, concentration of polymer solution, and centrifugation conditions. Figure S1 in the Supporting Information shows the absorption spectra of the neat polymers. Only PAMMA has strong absorbance in the region that overlaps SWNT spectral features. PNMA and PMMAFA do not interfere with the optical spectroscopy and so were not removed from SWNTs suspended in the supernatant solution prior to spectroscopy (Figure 2a and b). For the PAMMA separation agent, SWNTs in the supernatant solutions (Figure 2c) were filtered from solution and thoroughly washed with toluene to remove polymer before resuspension in SDBS solution for characterization.

Figure 2a–c shows the absorbance spectra of separated SWNTs (supernatant suspended, resuspended precipitate, and reference unseparated in SDBS solution) for each of the tested polymers. The CoMoCAT SWNTs have pronounced characteristic absorption bands at 400–510 nm for metallic species and at 510–1350 nm for semiconducting species. The bands at 800–1350 nm and 510–800 nm are due to S_{11} and S_{22}, respectively. The sharp absorbances at about 576 and 1000 nm are due to the S_{22} and S_{11} interband transitions of the (6,5) nanotube species.[38–40] The M_{11}/S_{22} peak-intensity ratio is used as a proxy for the relative content of met- and sem-SWNTs since S_{22} is less susceptible than S_{11} to environmental doping effects. The species content was roughly estimated from the area enclosed by the ''wiggles'' in the spectra since subtraction of the background of the SWNTs solution, whose intensity estimation can approximately be made[25] locally within each spectrum from the dips between the wiggles, is necessary.

Figure 2a shows that PNMA preferentially suspends met-SWNTs; the supernatant spectrum has a large M_{11} (≈480 nm) peak while the S_{22} band (≈576 nm) is dramatically suppressed with respect to the reference spectrum (as-received CoMoCAT SWNTs in SDBS solution). Correspondingly, the met-SWNT features are more suppressed in the PNMA-precipitate spectrum than the sem-SWNT features. Similar qualitative analysis of the spectra in Figure 2b and c indicates that PMMAFA and PAMMA preferentially suspend sem-SWNTs, which is obviously corroborated by the strong increase in met-SWNT (≈480 nm) absorption in the precipitates.

Another obvious feature of the enriched supernatant solutions, especially for PNMA and PMMAFA (Figure 2a and b), in contrast to the as-received SWNTs, is the redshift of the peak wavelengths, especially for the S_{11} peak at ≈1000 nm. For PAMMA separation (Figure 2c), the polymer was removed prior to spectroscopy and a substantial blueshift of the peaks in the supernatant spectrum was evident; before PAMMA removal, a redshift of peak wavelengths in the supernatant solution (Figure S2) was evident. The redshift might indicate large-diameter selectivity or the influence of the dispersion media environment. From the photoluminescence results discussed below, the large-diameter selectivity option can be eliminated.

2.2. Photoluminescence Excitation

Photoluminescence[41–43] excitation (PLE) maps (Figure 3) were used to characterize the chiral index (n,m) distributions

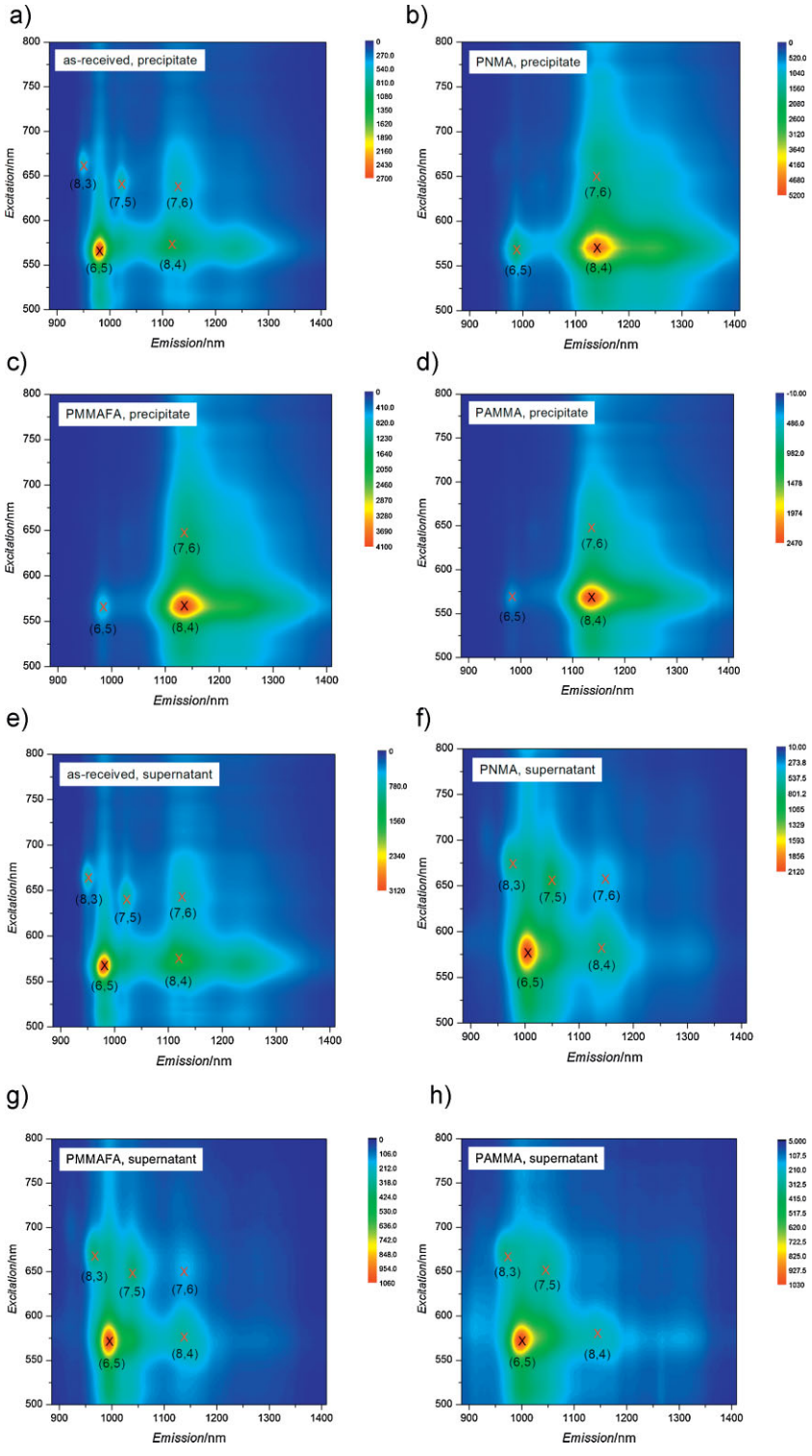

Figure 3. PLE maps of SWNTs dispersed with SDBS solution and of SWNTs after chemical separation. As-received CoMoCAT SWNTs dispersed using SDBS solution with a) precipitate fraction and e) supernatant fraction. CoMoCAT SWNT precipitates after separation in DMF with b) PNMA, c) PMMAFA, and d) PAMMA. CoMoCAT SWNTs in the supernatant solution after separation in DMF with f) PNMA, g) PMMAFA, and h) PAMMA.

of semiconducting SWNTs in the washed precipitates and in the supernatant solutions. As-received SWNTs dispersed in 1% SDBS solution in D_2O were also studied as a reference.

As-received CoMoCAT SWNTs (Figure 3a and e) are dominated by the (6,5) and (8,4) species. Also present with reasonably strong signals are the (8,3), (7,5), and (7,6) species. Figure 3a and e also indicates that SDBS shows no species selectivity. The polymer-separated precipitates (Figure 3b–d) exhibit similar modifications in their chiral distributions: the (6,5), (7,5), and (8,3) species PLE peaks are suppressed by all three polymers, indicating preferential suspension of these (with respect to (7,6) and (8,4)) in the supernatant solution. The preferentially suspended species (6,5), (8,3), and (7,5) are somewhat smaller (with $d_{tube} = 0.757$, 0.782, and 0.829 nm, respectively) than the precipitate species (8,4) and (7,6) ($d_{tube} = 0.840$ and 0.895 nm, respectively), which suggests a smaller size preference for dispersion by the polymers. Similar analysis of the PLE maps of the supernatant solution in Figure 3f–h confirms the preference for smaller-diameter species of all tested polymers. The selection mechanism is not plain from this data. The polymers may prefer tubes in a specific diameter range because of favorable binding energy. However, since the band gap E_{11} correlates closely (inversely) with the tube diameter, a preferential interaction between the polymers and SWNTs produced by a process related to the SWNTs' electronic structure is also compatible with our data. Whatever the underlying mechanism, it is apparent that the polymers prefer smaller-diameter tubes. Consequently, the redshift observed in the PNMA- and PMMAFA-suspended SWNTs UV/Vis/NIR spectra (Figure 2a and b, supernatant) should be attributed to the presence of unwashed polymer in the supernatant.

A subtle effect that could potentially confuse the interpretation of our PLE maps is the possibility of energy transfer from smaller tubes to larger tubes, which suppresses the small-tube emission in favor of the larger tubes.[44] If this is present in our data, it alters the interpretation of peak-height ratios within a single PLE map. This effect is presumably reproducible between maps provided that the sample processing conditions are comparable (as they are in this study) and so we are confident that changes in peak-height ratios between different PLE maps are a reliable proxy for changes in the underlying species distributions.

It is evident from both the UV/Vis/NIR absorbance spectra and the PLE maps that the species selectivity differs noticeably

NANO MICRO small

for the different polymers. Specifically, PMMAFA and PAMMA preferentially disperse sem-SWNTs but PNMA preferentially disperses met-SWNTs. All three polymers preferentially disperse smaller-diameter species.

We tentatively ascribe the polymers' species selectivity to their diameter selectivity, which dominates the SWNTs wrapping. Diameter selectivity in our study may result from the different polymer conformation, which is also believed to be influenced by the size and structure of the pendant functional groups as well as the solvent.[45,46] Solvent-dependent characteristics of the species selectivity, which will be discussed below, corroborate our suggested mechanism. UV/Vis/NIR spectra and PLE maps were employed to characterize the supernatant fraction of the separated SWNTs in different solvents (i.e., CH_3CN and $CHCl_3$). The standing time after sonication was set to be 2 weeks and only the polymer PNMA was tested as its species selectivity in DMF is different to that of the other two polymers.

The absorption spectra (Figure 4a and b) indicate that PNMA is selective to semiconducting species in both CH_3CN and $CHCl_3$. However, the PLE maps (Figure 4c and d) suggest that PNMA is selective to smaller-diameter species, mainly (6,5), in CH_3CN, while larger-diameter species, mainly (8,4) and (7,6), are preferred in $CHCl_3$. The different species selectivity of PNMA in various solvents is attributed to differing degrees of relaxation in the polymer conformation to the nanotube walls. The influence of the solvents on the conformation of PNMA was investigated using Hansen solubility parameters (HSP). Our prediction is made based on the group-contribution method[47] starting from poly(methyl methacrylate) (PMMA), which can be assumed to be the precursor of PNMA, due to the availability of its HSP both theoretically and experimentally. To simplify the estimation, we assume the contributions of the naphthyl and methyl side groups to the HSP of the corresponding polymers, which in our case are PNMA and PMMA, to be additive.[47] We also neglect the difference between the HSP of polymers and their repeating units so that we can conveniently calculate the HSP of PNMA directly from the HSP of PMMA by replacing the contribution of the methyl group with that of the naphthyl group. The HSP of PMMA and the group contributions, as well as the calculated HSP of PNMA, is listed in Table 1. The HSP of solvents[48] are listed in

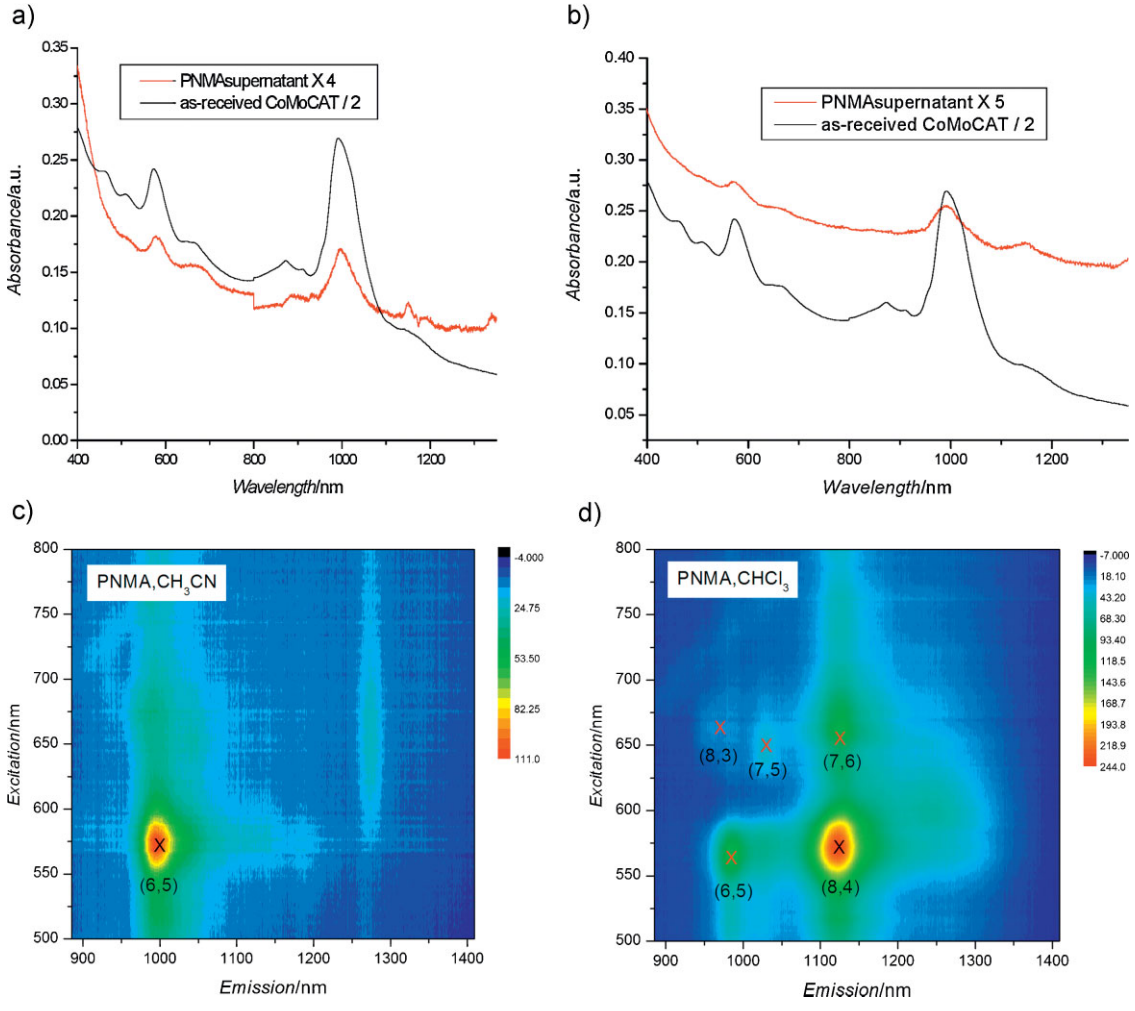

Figure 4. Solvent effects on the species selectivity of PNMA. UV/Vis/NIR absorbance spectra of the SWNTs in the supernatant fraction using a) CH_3CN (the concentration of PNMA in CH_3CN is ≈0.5%, limited by its solubility) and b) $CHCl_3$ as the solvent. PLE maps of the SWNTs in the supernatant fraction with solvents c) CH_3CN and d) $CHCl_3$. (Note: The black SWNT lines in (a) and (b) are spectra of the "as-received" SWNTs dispersed in D_2O/SDBS solution.)

Table 1. Hansen solubility parameters of polymers and group contributions.

Polymer/Functional Group	δ_D [$MPa^{1/2}$]	δ_P [$MPa^{1/2}$]	δ_H [$MPa^{1/2}$]
PMMA	18.81	10.22	8.59
$-CH_3$	−0.9714	−1.6448	−0.7813
Napathyl	2.0876	−3.7727	−2.3123
PNMA	21.869	8.0921	7.059

Table 2. Hansen solubility parameters of solvents and the expression, R_a, of the distances between solvent and PNMA.

Solvent	δ_D [$MPa^{1/2}$]	δ_P [$MPa^{1/2}$]	δ_H [$MPa^{1/2}$]	R_a^2 [$MPa^{1/2}$]
Acetonitrile	15.3	18.0	6.1	271.69
Dimethylformamide	17.4	13.7	11.3	129.32
Chloroform	17.8	3.1	5.7	92.99

Table 2 and the affinity between solvent and PNMA is expressed as the distance R_a[48] between the HSP of PNMA and those of solvents in Hansen space, which is calculated as $R_a^2 = 4(\delta_{D1}-\delta_{D2})^2 + (\delta_{P1}-\delta_{P2})^2 + (\delta_{H1}-\delta_{H2})^2$. The distance between PNMA and solvents increases in the order of chloroform, DMF, and acetonitrile. The affinity of the PNMA to different solvents increases in the order CH_3CN, DMF, and $CHCl_3$: $CHCl_3$ is the best solvent for PNMA and CH_3CN is the poorest. The diameter of the SWNTs suspended by PNMA in different solvents increases in the same order: $CHCl_3$ suspends the larger-diameter nanotubes. It seems that there is some direct relationship between PNMA's species selectivity and its affinities to solvents. In a poor solvent, the polymer conformation collapses to minimize the polymer exposure to the solvent. This would favor wrapping of the smaller-diameter species (6,5) in CH_3CN compared with $CHCl_3$ or DMF. In a good solvent, such as $CHCl_3$, the conformation of polymer is relaxed (i.e., looser) and larger-diameter species, such as (8,4) and (7,6), are thus preferentially suspended. The different behaviors of PNMA in different solvents suggest that its selectivity is explainable in part by a diameter preference, which arises from the energetics of polymer conformation change when complexing with the SWNT. However, comparison of the metallicity selectivity of different polymers in DMF indicates that the side groups do play an important role during the wrapping process. With naphthalene as the functional group, the polymer preferentially suspends metallic species while anthracene and fluorescein result in the polymers' selectivity to semiconducting species.

An interesting factor which is involved in the separation is light. In a control experiment, we repeated the experiments using the same setup of all experimental parameters except that, after sonication, we put the solutions in a dark area instead of a brightly lit area; in the ''dark'' experiments, no metallicity selectivity was observed in the UV/Vis/NIR spectra. We suggest that the presence of light will induce some dipole–dipole interaction between polymeric chromophores and SWNTs and it is this kind of dipole–dipole interaction that is responsible for the polymers' metallicity selectivity in DMF.[49,50] In experiments, photon-induced dipole–dipole interactions will possibly result in energy transfer between the units on which the dipoles reside.[51]

2.3. Fluorescence Spectra of Polymers

Energy transfer from polymeric chromophores to SWNTs can be characterized by the polymer fluorescence spectra. Fluorescence spectra of all polymers are shown in Figure 5a–c. To reduce the intermolecular interaction, low-polymer-concentration solutions were used in the fluorescence test. The separation process was repeated for all polymers in DMF and the fluorescence spectra of all polymers in the absence and presence of SWNTs were obtained. The concentrations of chromophores 2-naphthylmethacrylate (NMA), 9-anthracenyl-methyl-methacrylate (AMMA), and fluorescein-*o*-acrylate (FA) were 1.78×10^{-4}, 1.37×10^{-4}, and 1.3×10^{-5} mol L^{-1}, respectively. During the spectra collection, all variable parameters were set to be the same so that the fluorescence intensities are comparable.

From Figure 5a–c, the lower intensities in the presence of SWNTs suggests strong quenching in the presence of SWNTs for all polymers. In each figure, the difference (suppressed fraction of the spectra) between the original and quenched spectra was represented by the blue line, which was obtained by subtraction of the spectra of polymers in the presence of SWNTs from those in the absence of SWNTs. The disproportionality between the suppressed intensity and the original spectra indicates that it is unlikely to resolve the suppression by concentration variation since the chromophore concentration is in its linear range. This suggests the existence of some coupling interaction, such as energy transfer, between the polymer and SWNTs. Further evidence of energy transfer can be observed in a typical PLE map of suspended SWNTs in the undiluted 0.1% PAMMA/DMF solution. (Figure S4)

The different suppression tendency of the fluorescence for PNMA and PMMAFA/PAMMA suggests different interactions with SWNTs. For PNMA, the shorter-wavelength emission is more obviously suppressed, while suppression of longer-wavelength emission is more prominent for PMMAFA/PAMMA. The necessary condition of spectral overlap[51] between the fluorescence spectra of polymeric chromophores and the absorption spectra of SWNTs as well as the fact that energy transfer will occur more readily in the energetically favorable direction will ultimately determine the energy-transfer tendency. It is their interplay that determines the different fluorescence-quenching styles for PNMA and PMMAFA/PAMMA and results in their diverse metallicity selectivity. One concern about the above argument is that the energy transfer possibly *results from* rather than *will result in* the metallicity selectivity. Since we can observe the energy transfer immediately after sonication, we can eliminate the first possibility.

In our tested system, the interaction between SWNTs and aromatic functional groups is not limited to the van der Waals type, which is generated by thermal charge-distribution fluctuations. On the contrary, the induced dipole–dipole interaction may become involved in the presence of light. In

NANO MICRO small

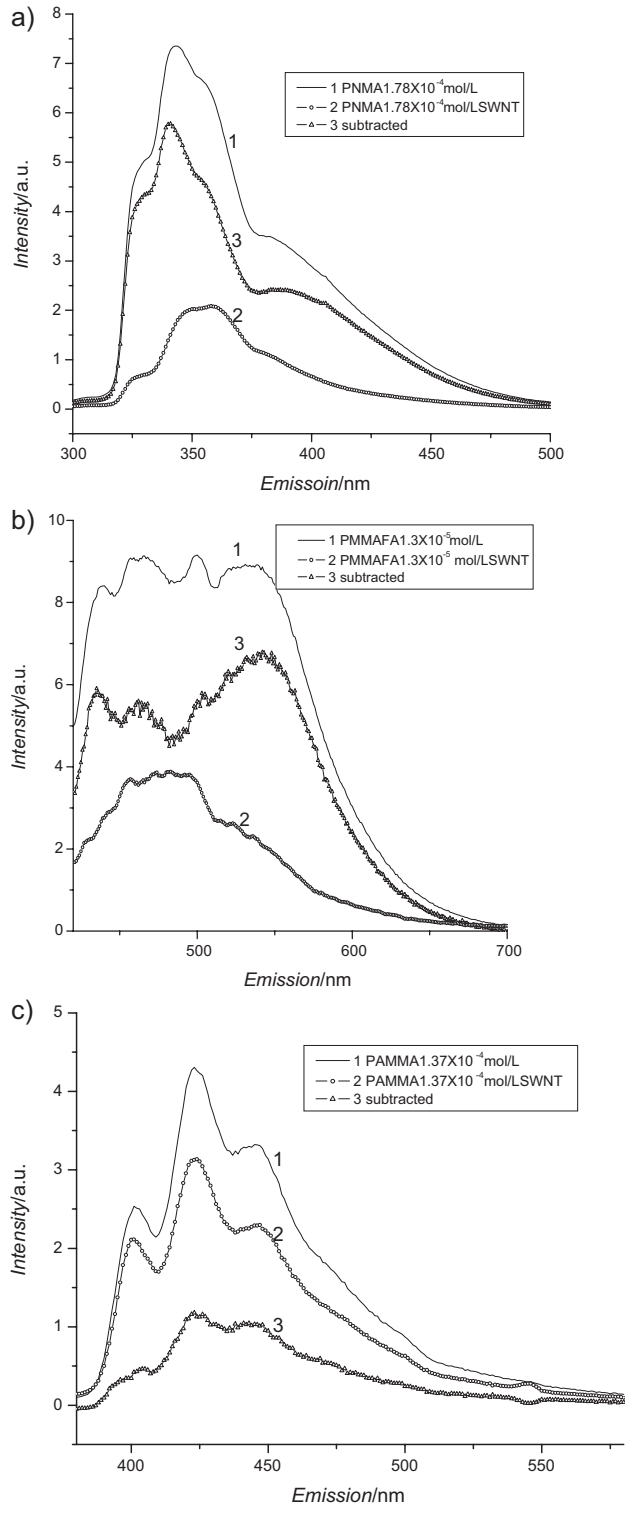

Figure 5. Fluorescence spectra of PNMA, PMMAFA, and PAMMA in the presence/absence of SWNTs. a) PNMA, b) PMMAFA, and c) PAMMA. (Note: Line 3 is obtained by subtracting Line 2 from Line 1.)

addition, the involvement of the polymer conformation change, which is enforced by the solvation in different solvents, complicates the situation. It is the interplay and relative magnitudes of all these kinds of weak interaction that results in the polymers' unique metallicity and diameter selectivity. Other factors such as structural compatibility (simultaneous optimization of the effective contact area and atomic correlation between SWNTs and aromatic groups) or electronic interaction[52,53] cannot be completely excluded from the contribution to the polymers' species discrimination and further investigation is required.

2.4. Electrical Measurement

To confirm the species enrichment, we fabricated short-channel thin-film FET devices using semiconductor-enriched SWNTs and characterized the electrical properties of the nanoelectronics. The solution used in the device fabrication was obtained by dispersing sem-SWNTs separated using PMMAFA in SDBS. For the preparation of electronic devices, we prefer to use supernatant because precipitates normally contain many bundles, which cannot be dispersed well into individual tubes.[54] Thin-film FETs were fabricated by the drop-casting method. A gate bias was applied to the underlying Si substrate, which served as the gate electrode, to modulate the carrier concentration in the SWNT network. The electrode configuration and typical device-performance plots are shown in Figure 6.

At least 90% of the devices (9 of 10) exhibited good FET performance with on/off ratios of about 10^3. This is much superior to the performance of devices made from the as-received SWNTs (1 of 10 devices showed an on/off ratio of $\approx$10 and the rest were <10; Figure S3), which confirms the enrichment of sem-SWNTs in the nanotube suspension. The relatively low on-state current may be limited by the low density of SWNTs in the channel, the lower current capacity of small-diameter SWNTs (preferentially selected by PMMAFA) compared with larger-diameter SWNTs, and possibly high Schottky barriers and nonohmic contacts.[55–57] The high ($\approx10^3$) FET on/off ratio corroborates our other evidence of species-selective enrichment. Further improvement in device performance can be anticipated by using larger-diameter SWNTs or higher-work-function electrodes since the on-state current can be substantially increased by lowering the Schottky barriers. The optimization of the electrode geometry and conditions for device fabrication will further improve the device performance.

The species selectivity is found to be quite sensitive to the polymer/solvent combinations. Different combinations show different discrimination between various SWNT species depending on their chiralities and diameters. Serial enrichment using multiple highly selective polymer/solvent combinations may provide higher purity and potentially even single-species enrichment.

Our method is scalable, nondestructive, compatible with SWNTs of different sources, iteratively repeatable, and affordable and thus makes widespread application possible according to Hersam's criteria.[58] Further improvement of FET device performance is anticipated through use of larger-diameter SWNTs or higher-work-function electrodes, as well as with optimization of electrode geometry and device-fabrication conditions.

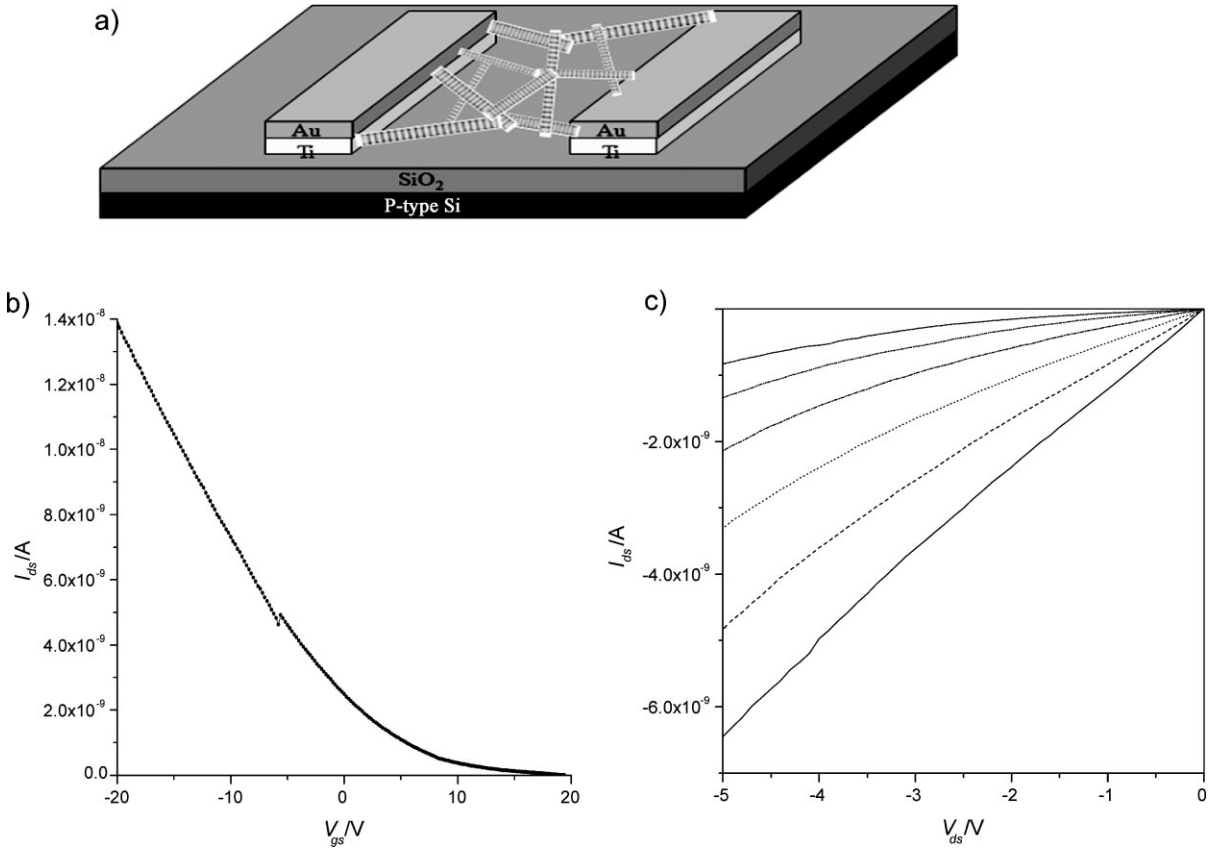

Figure 6. FET fabricated with sem-enriched SWNTs as the active channel using PMMAFA. a) Device configuration; b) Transfer characteristic (I_{ds}–V_{gs}) of a representative device at $V_{ds} = 2$ V; c) Current–voltage characteristics (I_{ds}–V_{ds}) of the device at V_{gs} ranging from −10 to 10 V with a step of 4 V from bottom to top.

3. Conclusions

Three novel polymethacrylates, PNMA, PAMMA and PMMAFA, with pendant aromatic functional groups have been successfully employed in the separation of SWNTs according to their electronic properties (met-/sem-) and diameters and highly effective enrichment has been achieved. Optical absorbance spectra and PLE maps indicate that this family of polymers has strong selectivity towards certain SWNT species with specific diameters and that the species selectivity is highly sensitive to the polymer/solvent combination. Specifically, DMF, PMMAFA, and PAMMA preferentially disperse semiconducting SWNTs while PNMA preferentially disperses metallic SWNTs. All three polymers preferentially disperse small-diameter SWNTs in DMF. The selectivity of PNMA (to metallic species in DMF) is sensitive to the solvent employed. In CH_3CN, PNMA is selective to smaller-diameter semiconducting species while larger-diameter semiconducting species are preferentially suspended in $CHCl_3$. The solvent effects on species selectivity suggest the mechanism of diameter selectivity, which results from a change of polymer conformation. The change of the polymer fluorescence in the presence of SWNTs was tracked and the involvement of photons in the enrichment process was identified, with the photon-induced dipole–dipole interaction probably responsible for the metallicity selectivity in DMF. The diverse selective behavior of these polymers results from the interplay between photon-induced dipole–dipole interaction and polymer-conformation change. Other kinds of weak interactions, such as van der Waals interactions as well as structural compatibility, also cannot be excluded.

The successful fabrication of thin-film FET devices with a semiconductor-enriched solution has also been demonstrated. The reproducible on/off ratio of about 10^3 in these devices confirms the enrichment in semiconducting species.

4. Experimental Section

Materials: CoMoCAT SWNTs were purchased from SouthWest Nanotechnologies, Inc. and were used as received. The polymers PNMA, PAMMA, and PMMAFA, as well as SDBS, were obtained from Aldrich and were used as received. The solvents, *N*,*N*-DMF, toluene, and deuterium oxide (D_2O), were purchased from Sino Chemical Company Pte Ltd. and were used without further purification, except as specified elsewhere.

SWNT separation with polymers: Separation was carried out by suspending as-received SWNTs (2 mg) in polymer solution in DMF (10 mL). After sonication for 10 min at 175W and standing for 2 weeks, followed by centrifugation at 20 000 *g* for 1 h, both the

NANO MICRO small

upper 90% of the supernatant and the precipitate were collected for further experiments. The standing periods between the sonication and centrifugation were set to be 2 weeks for all separations to remove the standing time as a possible variable affecting the measured enrichment.

UV/Vis/NIR absorbance spectra of SWNTs separated in the supernatant solutions were obtained directly from the supernatant, except in the case of PAMMA, in which absorbance bands of polymer and SWNTs badly overlap (Figure S1). Polymer-wrapped precipitated SWNTs were thoroughly washed with toluene. The clean SWNT powders were redispersed in 1% SDBS/D_2O solution and then centrifuged (at 57 000 *g*) prior to UV/Vis/NIR and photoluminescence spectroscopy scans.

Polymer-dispersed supernatant SWNTs were thoroughly washed with toluene to remove polymer before use in device fabrication.

Characterization techniques: UV/Vis/NIR spectra of SWNT solutions were recorded on a Cary 5000 UV/Vis/NIR spectrophotometer. 0.1% polymer solution was used as reference for background subtraction for PNMA- and PMMAFA-suspended supernatant SWNTs; 1% SDBS in D_2O was used for other supernatant SWNTs scans. No background subtraction of polymer absorption was applied to the UV/Vis/NIR spectra of the precipitates because the toluene washing strongly suppressed the polymer absorption features (Figure S2). Some spectra have been magnified for comparison; this has no effect on the content ratio of different species. Some spectra exhibit a sharp edge at almost exactly 800 nm due to the change of the detector during data collection.

PLE measurements of the supernatant SWNTs suspended in the polymer solution as well as the precipitates resuspended in SDBS were performed on a Jobin-Yvon Nanolog-3 spectrofluorometer with an InGaAs detector. For the supernatant scans of PMMAFA- and PAMMA-suspended nanotubes, due to the redshift of the fluorescence band resulting from the formation of excimer at higher concentrations, the solutions were diluted to avoid the excitation of the polymer in our wavelength region of interest so that the unfavorable energy transfer can be eliminated.

Fluorescence spectra of the polymer solutions in a 1-cm quartz cell were collected with an AMINCO BOWMAN II luminescence spectrometer. The excitation wavelengths were 278, 269, and 276 nm for PNMA, PAMMA, and PMMAFA, respectively.

Back-gated SWNT FETs were fabricated on heavily doped p-type silicon wafers capped with 300-nm thermally grown silicon dioxide layers. The source and drain electrodes were made of 10-nm-thick Ti and 60-nm-thick Au by photolithography. The heavily doped p-type silicon was used as the back gate. The width and length of the channel were 100 and 20 μm, respectively. All electrical measurements were carried out at ambient conditions using a Keithley semiconductor parameter analyzer Model 4200-SCS.

Acknowledgements

The work was supported by a Competitive Research Program grant from the Singapore National Research Foundation (NRF-CRP2-2007-02). X.P. acknowledges the support of Nanyang Technological University through a Research Scholarship.

[1] S. Iijima, *Nature* **1991**, *354*, 56–58.
[2] T. Durkop, S. A. Getty, E. Cobas, M. S. Fuhrer, *Nano Lett.* **2004**, *4*, 35–39.
[3] K. Bradley, J. C. P. Gabriel, G. Gruner, *Nano Lett.* **2003**, *3*, 1353–1355.
[4] Q. Cao, H. S. Kim, N. Pimparkar, J. P. Kulkarni, C. J. Wang, M. Shim, K. Roy, M. A. Alam, J. A. Rogers, *Nature* **2008**, *454*, 495–500.
[5] Y. X. Zhou, A. Gaur, S. H. Hur, C. Kocabas, M. A. Meitl, M. Shim, J. A. Rogers, *Nano Lett.* **2004**, *4*, 2031–2035.
[6] Q. Cao, J. A. Rogers, *Adv. Mater.* **2009**, *21*, 29–53.
[7] P. Avouris, *Acc. Chem. Res* **2002**, *35*, 1026–1034.
[8] R. Saito, M. Fujita, G. Dresselhaus, M. S. Dresselhaus, *Appl. Phys. Lett.* **1992**, *60*, 2204–2206.
[9] Y. M. Li, D. Mann, M. Rolandi, W. Kim, A. Ural, S. Hung, A. Javey, J. Cao, D. W. Wang, E. Yenilmez, Q. Wang, J. F. Gibbons, Y. Nishi, H. J. Dai, *Nano Lett.* **2004**, *4*, 317–321.
[10] H. J. Huang, R. Maruyama, K. Noda, H. Kajiura, K. Kadono, *J. Phys. Chem. B* **2006**, *110*, 7316–7320.
[11] C. M. Yang, J. S. Park, K. H. An, S. C. Lim, K. Seo, B. Kim, K. A. Park, S. Han, C. Y. Park, Y. H. Lee, *J. Phys. Chem. B* **2005**, *109*, 19242–19248.
[12] R. Krupke, F. Hennrich, H. von Lohneysen, M. M. Kappes, *Science* **2003**, *301*, 344–347.
[13] D. S. Lee, D. W. Kim, H. S. Kim, S. W. Lee, S. H. Jhang, Y. W. Park, E. E. B. Campbell, *Appl. Phys. A* **2005**, *80*, 5–8.
[14] T. Lutz, K. J. Donovan, *Carbon* **2005**, *43*, 2508–2513.
[15] M. Zheng, A. Jagota, M. S. Strano, A. P. Santos, P. Barone, S. G. Chou, B. A. Diner, M. S. Dresselhaus, R. S. McLean, G. B. Onoa, G. G. Samsonidze, E. D. Semke, M. Usrey, D. J. Walls, *Science* **2003**, *302*, 1545–1548.
[16] M. Zheng, E. D. Semke, *J. Am. Chem. Soc.* **2007**, *129*, 6084–6085.
[17] M. S. Arnold, A. A. Green, J. F. Hulvat, S. I. Stupp, M. C. Hersam, *Nat. Nanotechnol.* **2006**, *1*, 60–65.
[18] M. S. Strano, C. A. Dyke, M. L. Usrey, P. W. Barone, M. J. Allen, H. W. Shan, C. Kittrell, R. H. Hauge, J. M. Tour, R. E. Smalley, *Science* **2003**, *301*, 1519–1522.
[19] C. Menard-Moyon, N. Izard, E. Doris, C. Mioskowski, *J. Am. Chem. Soc.* **2006**, *128*, 6552–6553.
[20] L. An, Q. A. Fu, C. G. Lu, J. Liu, *J. Am. Chem. Soc.* **2004**, *126*, 10520–10521.
[21] W. J. Kim, M. L. Usrey, M. S. Strano, *Chem. Mater.* **2007**, *19*, 1571–1576.
[22] T. Hemraj-Benny, S. S. Wong, *Chem. Mater.* **2006**, *18*, 4827–4839.
[23] Y. Maeda, S. Kimura, M. Kanda, Y. Hirashima, T. Hasegawa, T. Wakahara, Y. F. Lian, T. Nakahodo, T. Tsuchiya, T. Akasaka, J. Lu, X. W. Zhang, Z. X. Gao, Y. P. Yu, S. Nagase, S. Kazaoui, N. Minami, T. Shimizu, H. Tokumoto, R. Saito, *J. Am. Chem. Soc.* **2005**, *127*, 10287–10290.
[24] D. Chattopadhyay, L. Galeska, F. Papadimitrakopoulos, *J. Am. Chem. Soc.* **2003**, *125*, 3370–3375.
[25] Z. H. Chen, X. Du, M. H. Du, C. D. Rancken, H. P. Cheng, A. G. Rinzler, *Nano Lett.* **2003**, *3*, 1245–1249.
[26] H. P. Li, B. Zhou, Y. Lin, L. R. Gu, W. Wang, K. A. S. Fernando, S. Kumar, L. F. Allard, Y. P. Sun, *J. Am. Chem. Soc.* **2004**, *126*, 1014–1015.
[27] Z. B. Zhang, S. L. Zhang, *J. Am. Chem. Soc.* **2007**, *129*, 666–671.
[28] S. Y. Ju, J. Doll, I. Sharma, F. Papadimitrakopoulos, *Nat. Nanotechnol.* **2008**, *3*, 356–362.
[29] R. J. Chen, Y. G. Zhang, D. W. Wang, H. J. Dai, *J. Am. Chem. Soc.* **2001**, *123*, 3838–3839.
[30] V. Georgakilas, K. Kordatos, M. Prato, D. M. Guldi, M. Holzinger, A. Hirsch, *J. Am. Chem. Soc.* **2002**, *124*, 760–761.

[31] K. A. S. Fernando, Y. Lin, W. Wang, S. Kumar, B. Zhou, S. Y. Xie, L. T. Cureton, Y. P. Sun, *J. Am. Chem. Soc.* **2004**, *126*, 10234–10235.
[32] H. M. So, B. K. Kim, D. W. Park, B. S. Kim, J. J. Kim, K. J. Kong, H. J. Chang, J. O. Lee, *J. Am. Chem. Soc.* **2007**, *129*, 4866–4867.
[33] M. C. LeMieux, M. Roberts, S. Barman, Y. W. Jin, J. M. Kim, Z. N. Bao, *Science* **2008**, *321*, 101–104.
[34] W. Wang, K. A. S. Fernando, Y. Lin, M. J. Meziani, L. M. Veca, L. Cao, P. Zhang, M. M. Kimani, Y. P. Sun, *J. Am. Chem. Soc.* **2008**, *130*, 1415–1419.
[35] A. Nish, J. Y. Hwang, J. Doig, R. J. Nicholas, *Nat. Nanotechnol.* **2007**, *2*, 640–646.
[36] J. Y. Hwang, A. Nish, J. Doig, S. Douven, C. W. Chen, L. C. Chen, R. J. Nicholas, *J. Am. Chem. Soc.* **2008**, *130*, 3543–3553.
[37] F. M. Chen, B. Wang, Y. Chen, L. J. Li, *Nano Lett.* **2007**, *7*, 3013–3017.
[38] F. Hennrich, R. Krupke, S. Lebedkin, K. Arnold, R. Fischer, D. E. Resasco, M. Kappes, *J. Phys. Chem. B* **2005**, *109*, 10567–10573.
[39] M. J. O'Connell, S. M. Bachilo, C. B. Huffman, V. C. Moore, M. S. Strano, E. H. Haroz, K. L. Rialon, P. J. Boul, W. H. Noon, C. Kittrell, J. P. Ma, R. H. Hauge, R. B. Weisman, R. E. Smalley, *Science* **2002**, *297*, 593–596.
[40] S. M. Bachilo, M. S. Strano, C. Kittrell, R. H. Hauge, R. E. Smalley, R. B. Weisman, *Science* **2002**, *298*, 2361–2366.
[41] R. B. Weisman, S. M. Bachilo, *Nano Lett.* **2003**, *3*, 1235–1238.
[42] M. Jones, C. Engtrakul, W. K. Metzger, R. J. Ellingson, A. J. Nozik, M. J. Heben, G. Rumbles, *Phys. Rev. B* **2005**, *71*, 115426.
[43] Y. Miyauchi, M. Oba, S. Maruyama, *Phys. Rev. B* **2006**, *74*, 205440.
[44] L. J. Li, M. Glerup, A. N. Khlobystov, J. G. Wiltshire, J. L. Sauvajol, R. A. Tavlor, R. J. Nicholas, *Carbon* **2006**, *44*, 2752–2757.
[45] R. Traiphol, P. Sanguansat, T. Srikhirin, T. Kerdcharoen, T. Osotchan, *Macromolecules* **2006**, *39*, 1165–1172.
[46] S. Y. Quan, F. Teng, Z. Xu, L. Qian, Y. B. Hou, Y. S. Wang, X. R. Xu, *Eur. Polym. J.* **2006**, *42*, 228–233.
[47] E. Stefanis, C. Panayiotou, *Int. J. Thermophys.* **2008**, *29*, 568–585.
[48] C. M. Hansen, *Hansen Solubility Parameters: A User's Handbook*, CRC Press, Boca Raton, Florida **2000**.
[49] Y. Itoh, O. Yamashita, A. Hachimori, M. Kojima, S. Suzuki, *J. Polym. Sci. Part A: Polym. Chem.* **1995**, *33*, 137–142.
[50] D. A. Holden, X. X. Ren, J. E. Guillet, *Macromolecules* **1984**, *17*, 1500–1504.
[51] Valeur. Bernard, *Molecular Fluorescence: Principles and Applications*, Wiley-VCH, Weinheim, Germany **2001**.
[52] J. Lu, S. Nagase, X. W. Zhang, D. Wang, M. Ni, Y. Maeda, T. Wakahara, T. Nakahodo, T. Tsuchiya, T. Akasaka, Z. X. Gao, D. P. Yu, H. Q. Ye, W. N. Mei, Y. S. Zhou, *J. Am. Chem. Soc.* **2006**, *128*, 5114–5118.
[53] J. Lu, L. Lai, G. Luo, J. Zhou, R. Qin, D. Wang, L. Wang, W. N. Mei, G. Li, Z. Gao, S. Nagase, Y. Maeda, T. Akasaka, D. Yu, *Small* **2007**, *3*, 1566–1576.
[54] C. W. Lee, C. H. Weng, L. Wei, Y. Chen, M. B. Chan-Park, C. H. Tsai, K. C. Leou, C. H. P. Poa, J. L. Wang, L. J. Li, *J. Phys. Chem. C* **2008**, *112*, 12089–12091.
[55] W. Kim, A. Javey, R. Tu, J. Cao, Q. Wang, H. J. Dai, *Appl. Phys. Lett.* **2005**, *87*, 173101.
[56] A. Javey, J. Guo, Q. Wang, M. Lundstrom, H. J. Dai, *Nature* **2003**, *424*, 654–657.
[57] L. Zhang, S. Zaric, X. M. Tu, X. R. Wang, W. Zhao, H. J. Dai, *J. Am. Chem. Soc.* **2008**, *130*, 2686–2691.
[58] M. C. Hersam, *Nat. Nanotechnol.* **2008**, *3*, 387–394.

Received: December 31, 2009
Revised: March 31, 2010
Published online: May 19, 2010

